Journal of Microbiology Research 2025, 15(1): 7-16
DOI: 10.5923/j.microbiology.20251501.02

Comparative Evaluation of Antimicrobial Activities of Biogenic Silver Nanoparticles Synthesized from Tropical Fruit Components

Bright Ankudze

University of Education, Winneba, Ghana

Abstract Extracts from plants are known to possess crucial phytochemicals essential for reduction and stabilization of nanoparticles. Phytochemicals can increase the potency of the nanoparticles and widen their scope of application. Studies have shown that nanoparticles behave differently when prepared with different plants extracts. Hence, comparative study of different biogenically prepared nanoparticles can increase understanding of the effect of surface functionalization in selective antimicrobial activity and potency of nanoparticles. In a previous studies, different silver nanoparticles were prepared using *Chrysophyllum albidum* peel (Alb-AgNPs), *Cyperus esculentus* tuber (CpE-AgNPs), and *Dialium cochinchinense* (VeV-AgNPs) husk. In the present study, a comprehensive comparison is made among the prepared silver nanoparticles to ascertain their antimicrobial efficacy. The result showed that VeV-AgNPs had the strongest activity, with minimum inhibitory concentrations as low as 3.9 μg/mL against *E. coli*, and synergistic effects with ciprofloxacin. Alb-AgNPs exhibited broad-spectrum efficacy, notably against *E. coli* and *C. albicans*, and enhanced antibiotic activity, whereas CpE-AgNPs demonstrated moderate effects but strong synergy at low doses and broader spectrum against wider range of microorganism. In antibiofilm assays, CpE-AgNPs were highly effective against *S. mutans* and *MRSA* at low concentrations, Alb-AgNPs showed consistent but dose-dependent inhibition, and VeV-AgNPs showed ability to significantly disrupt preformed biofilms across bacterial and fungal strains.

Keywords Silver nanoparticles, Green synthesis, Phytochemicals, Antimicrobial activity, Biofilm inhibition, Synergistic effect

1. Introduction

The advancement of medicine has led to numerous breakthroughs in the fight against difficult-to-treat and emerging diseases through the development of highly potent antiviral and antimicrobial agents [1-7]. Over the years, nanotechnology has emerged as a transformative field with wide-ranging applications in medicine [8], agriculture, food preservation, and environmental remediation [9,10]. Among the various nanomaterials, silver nanoparticles (AgNPs) have received particular attention owing to their remarkable antimicrobial [11], antioxidant [12], and catalytic properties [13]. The synthesis of AgNPs can be achieved through physical, chemical, or biological approaches. Physical methods such as laser ablation and evaporation-condensation [14], and chemical reduction using stabilizing agents [15], allow fine control over particle size and morphology, however, they are often limited by high energy demands and the generation of toxic by-products. Biological or green synthesis, on the other hand, offers a sustainable and eco-friendly alternative, relying on natural biomolecules to drive nanoparticle formation [16].

Green synthesis leverages the reducing and stabilizing agents present in plant [17], algal [18], fungal [19], and animal-derived extracts, which replace harsh chemical reagents with biogenic molecules. Plant-derived extracts, in particular, are rich in phenolics, flavonoids, terpenoids, alkaloids, and polysaccharides, all of which facilitate both the reduction of metal ions and the stabilization of the resulting nanoparticles [20]. Leaves and fruit peels from species such *as Azadirachta indica* (neem), *Medicago sativa* [21], *Coriandrum sativum* [22], rice [23], and cabbage [24], have been widely used for the biosynthesis of nanoparticles, producing stable nanostructures under mild conditions. Beyond plants, algal and fungal extracts provide enzymatic pathways that influence particle size and morphology, while animal-derived materials such as proteins (egg white, milk casein, gelatin, collagen, silk fibroin), polysaccharides (chitosan), and natural products like honey act as templates

* Corresponding author:
ankudzeb@gmail.com (Bright Ankudze)
Received: Sep. 17, 2025; Accepted: Oct. 8, 2025; Published: Oct. 25, 2025
Published online at http://journal.sapub.org/microbiology

or stabilizers, yielding biocompatible nanoparticles with diverse applications [25].

Biologically mediated nanostructures are increasingly being explored across multiple sectors. In environmental remediation, they play roles in dye degradation, pollutant removal, and photocatalysis [25]. In agriculture, they serve as nano-fertilizers, seed priming agents, and nano-pesticides that enhance nutrient use efficiency and plant resilience [25]. In medicine, their potential as antimicrobial coatings, wound dressings, targeted drug delivery systems [26,27], and cancer theranostics has gained significant momentum. The versatility of these applications underscores the importance of synthesis methods and precursor biomaterials in determining the physicochemical properties and functional performance of AgNPs.

Despite the versatility and wider application of green synthesized nanoparticles, growing concerns about the climate crisis have highlighted the need for more sustainable and environmentally friendly approaches in green synthesis of silver nanoparticles [28]. Significant strides have been made to make nanomaterial synthesis greener, with particular attention to replacing heavily dependent biomaterials with less-used or discarded bioresources. The use of discarded plant waste as precursor materials for nanoparticle synthesis provides an added layer of significance [29]. They do not only help reduce environmental pollution but also offers a low-cost, eco-friendly pathway for producing valuable nanomaterials. As a result, much effort has gone into advocating the use of discarded plant wastes such as fruit peels, seed shells, vegetable residues [30] and agro-biomass [23] for the green synthesis of silver nanoparticles.

Among promising discarded wastes, peels of *Chrysophyllum albidum* and husks of *Dialium cochinchinense* have a rich phytochemical composition and widespread availability. Peels of *Chrysophyllum albidium* have nutritional and therapeutic properties, and can be used for green synthesis of AgNPs, yielding nanoparticles with strong antibacterial and antibiofilm activity. Husk of *Dialium cochinchinense* [31–33] traditionally consumed for its sweet-sour pulp and used in ethnomedicine, has also been successfully applied in nanoparticle synthesis using discarded fruit husks under sunlight exposure, producing effective antimicrobial agents. Another widely available plant resource, especially in the tropical regions that have been explored for biogenic synthesis of silver nanoparticles is tiger nuts [34]. Tiger nut (*Cyperus esculentus*) tubers are nutritionally dense, containing oils, starch, fibre, and polyphenolics, which have been linked to health benefits and, more recently, have been exploited for AgNP synthesis with notable antimicrobial outcomes [35]. As different biomaterials provide unique phytochemicals that act as reducing and capping agents, comparative studies that evaluate nanoparticles synthesized from diverse biomaterials are therefore essential to identify the most effective synthesis pathways and selective performance for targeted application. Such studies are particularly relevant in the current era, where antimicrobial resistance poses a pressing global health challenge.

In previous studies, silver nanoparticles were synthesized using different extracts from *Cyperus esculentus* [35] tubers, *Chrysophyllum albidum* [36] peels, and *Dialium cochinchinense* [37] husks as reducing and stabilizing agents. The obtained silver nanoparticles were studied for their antimicrobial properties. In the present study, a comparative evaluation of nanoparticles derived from *Cyperus esculentus*, *Chrysophyllum albidum*, and *Dialium cochinchinense* was presented. This comparative study is crucial to determine their relative antimicrobial performance and identify the most promising candidates for practical application.

2. Experimental

2.1. Chemicals

Silver nitrate ($AgNO_3$, Merck, ≥ 99 %) was used as a precursor for the synthesis of silver nanoparticles. *Chrysophyllum albidum*, *Cyperus esculentus*, *Dialium cochinchinense* fruits were used as reducing agents in separate synthesis to prepare different sets of silver nanoparticles. The fruits were purchased from the local market. Hypochlorite solution was used to disinfect the *Chrysophyllum albidum* fruit peel, *Dialium cochinchinense*, and *Cyperus esculentus* fruit before use. Methanol (Sigma Aldrich, analytical grade), Phosphate buffer saline (PBS), Mueller-Hinton Broth (Oxoid, USA), MTT (3-(4,5- dimethylthiazole-2-yl)-2,5-diphenyltetrazolium bromide, 0.1%, w/v, Sigma Aldrich), Phosphate Buffered Saline (PBS, Sigma Aldrich, analytical grade), McFarland standard (barium chloride and sulphuric acid) were used to study the antimicrobial properties of the prepared silver nanoparticles.

2.2. Synthesis of AgNPs

Three different silver nanoparticles were prepared, namely: CpE-AgNPs, Alb-AgNPs and VeV-AgNPs using *Cyperus esculentus*, *Chrysophyllum albidum* and *Dialium cochinchinense* as bio-reducing and stabilizing agents. Each bio material was used as a reducing agent to prepare one type of silver nanoparticles. In all, three different types of silver nanoparticle were prepared using the different bio-reducing agents. First extracts were prepared by soaking 7g, 1g and 2.5g of *Cyperus esculentus* tuber, *Chrysophyllum albidum* dried peels and *Dialium cochinchinense* husk, respectively, in 40 mL of water for 24 hours. To prepare the AgNPs, 40 mL of extracts were mixed with 2 mL of 0.01 M $AgNO_3$, stirred, and exposed to sunlight. The formation of the AgNPs were observed a color change from colourless, pale-yellow and pale yellow, to dark red for extract obtained from *Cyperus esculentus* tuber, *Chrysophyllum albidum* dried peels and *Dialium cochinchinense* husk, respectively. After centrifugation, the particles were separated and stored for further analysis.

2.3. Characterization of Prepared AgNPs

The synthesized AgNPs were characterized using: UV-Vis spectrophotometer to confirm plasmonic absorption. Scanning electron microscopy (SEM) for morphological analysis. X-ray diffraction (XRD) to determine crystallinity.

Fourier-transform infrared spectroscopy (FTIR) to identify functional groups involved in stabilization.

2.4. Test Organisms

The microorganisms used as test organisms for the study include Methicillin-Resistant *Staphylococcus aureus* (NCTC 29212), *Candida albicans* (ATCC 90028), *Aspegillus niger* (ATCC 6275), *Klebsiella pneumoniae* (NCTC 13440), *Salmonella typhi* (ATCC14028), *Streptococcus mutans* (ATCC 700610), *Pseudomonas aeruginosa* (ATCC 4853) and *Escherichia coli* (ATCC25922).

2.5. Determination of Antimicrobial Activity

To evaluate the antimicrobial properties of CpE-AgNPs, Alb-AgNPs and VeV-AgNPs, the broth micro-dilution method was employed using a 96 well microtiter plates according to previously established procedure (Clinical and Laboratory Standard Institute, [38]. For this study, 1 mg/mL AgNPs were prepared from each of the different silver nanoparticles. The preparation involved dispensing 100 µL of double-strength Mueller-Hinton broth into each well of a 96-well plate, which was then mixed with 100 µL AgNPs to create well concentrations ranging from 250.0 –0.1 mg/mL using the stock solution, resulting in ten different concentrations. For each column in the microtiter plate, wells 11 and 12 were utilized as the positive control (Broth + organism only) and negative control (Broth with no organism), respectively, for each microbial strain. Similarly, separate plates were prepared for antibiotics, namely ciprofloxacin, tetracycline, ampicillin, ketoconazole, fluconazole, and nystatin, and their concentrations were varied from 128.0 – 0.125 µg/mL, against all test bacteria and fungi. Subsequently, 100 µL of each of the 0.5 McFarland standard was added to the test organisms and the plates were then incubated at 37 ℃ for 24-48 hours for bacterial and fungal strains, respectively. The minimum inhibitory concentrations (MICs) were determined by visual examination following the addition of tetrazolium chloride (TTC) dye at a concentration of 0.1 g/mL after 10 minutes. The MICs were determined as the lowest concentration that did not change color from colorless/light yellow to red/pink.

2.6. Minimum Bactericidal (MBC) and Fungicidal Concentration (MFC) Determination

To investigate the microbial cell-killing potential (bactericidal/fungicidal effect) of the AgNPs, the minimum bactericidal/fungicidal concentrations (MBC/MFC) were determined. For this, samples from each well of the susceptibility testing assays were transferred onto sterile nutrient agar plates and incubated for 24/48 hours at 37 ℃ for bacteria/fungi, respectively. After incubation, the plates were examined for the presence or absence of growth on the nutrient agar (Nester et al. 2004).

2.7. Evaluation of Synergistic Effects of the Test AgNPs and Antibiotics

The combinatory effects of the AgNPs and antimicrobial orthodox drugs were studied against the test microbes using the checkerboard method, with minor modifications based on previous studies by Khodavandi et al. (2010) and Nascimento Da Silva et al. (2013). In brief, solutions with various proportions of AgNPs and drugs (final volume of 200 µL) were prepared from twice the MIC solutions of each test sample and individual antibiotics (1 mg/mL). The antimicrobial activity of these solutions was determined, as described for MIC determination. The Fractional Inhibitory Concentration index (FICI) was calculated using *equation (1).*

$$FICI = \left(\frac{MICA+S}{MICA}\right) + \left(\frac{MICS+A}{MICS}\right) \quad (1)$$

where MICA+S refers to the lowest amount of antibiotic required in combination with AgNPs sample to inhibit bacterial growth, while MICS+A represents the lowest concentration of AgNPs sample in combination with an antibiotic, the minimum inhibitory concentrations of antibiotics and AgNPs are represented with MICA and MICS, respectively. The interaction between AgNPs and antibiotics is categorized as synergistic if the FIC Index ≤ 0.5, partially synergistic if the FIC Index is > 0.5 and < 1, additive if the FIC Index is = 1, no difference if the FIC Index is >1 and ≤ 4, and antagonistic if the FIC Index is greater > 4.0.

2.8. Determination of Anti-Biofilm Formation Activity of the Prepared AgNPs

The antibiofilm activity of the *AgNPs* against the selected microorganisms was studied using the protocol by Pierce et al. (2008) with little modification. In brief, about 50 µL of MHB was added to each well of a flat 96-well microtiter plate. The different AgNPs samples (50 µL) were serially diluted to obtain concentration within the range of 500 to 0.197 µg/mL. Afterwards, the microbial suspensions (50 µL, 2×10^6 cells/mL) were added to wells of columns 1-11, and the plates were incubated for 24 h at 37 ℃. After the incubation, the liquid was removed with a pipette without disturbing the biofilm. PBS (100 µL) was used twice to wash away and remove any planktonic and non-adherent cells. The postprocessing to quantify the metabolic activity after the antimicrobial treatment were checked by XTT reduction assay as previously described by Pierce et al. (2008) with slight modifications. The microtiter plates were then read at 490 nm using a spectrophotometer. The procedure was repeated three times. The potential of each of the *AgNPs* samples to reduce the optical density compared to the negative control was noted as the biofilm inhibitory activity as described by equation (2).

$$\%\ \text{biofilm inhibition} = \left(1 - \frac{\text{OD of treatment}}{\text{OD of control}}\right) \times 100 \quad (2)$$

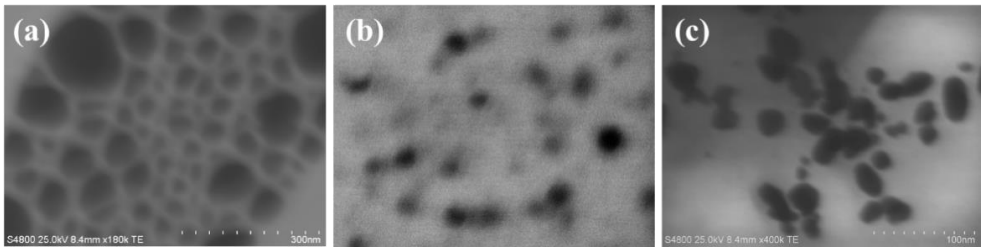

Figure 1. STEM images of (a) Alb-AgNPs (b) CpE-AgNPs, (c) VeV-AgNPs

Table 1. Structural properties of VeV-AgNPs, Alb-AgNPs and CpE-AgNPs

Nanoparticle	Size range / Mean size	Morphology	Reaction time and conditions	Plasmonic absorption (UV–Vis)	Major functional groups (FTIR)
VeV-AgNPs (*Dialium cochinchinense*)	20–54 nm / ~45.0 ±8.5 nm	Quasi-spherical (dominant), occasional rods	Rapid under sunlight (~5 min); slower under ambient	~455 nm	O–H, C=O, C=C, C–O
Alb-AgNPs (*Chrysophyllum albidum* peel)	28–90 nm (some >100 nm)	Quasi-spherical, polydisperse	Sunlight: ~5 min; Ambient: ~4 h	~434 nm	O–H, C=O, C=C, C–O, C–N
CpE-AgNPs (*Cyperus esculentus* tuber)	50–80 nm	Quasi-spherical, spherical, occasional rods	Rapid under sunlight (~5 min), slower under ambient	~450 nm	C=O, C–H (alkene), C–N

3. Results and Discussion

3.1. Structural Studies of Alb-AgNPs, VeV-AgNPs and CpE-AgNPs

The morphology of the prepared silver nanoparticles was observed using scanning electron microscope. It can be observed in Figure 1 that Alb-AgNPs were quasi-spherical but polydisperse, with a broader size range (28–90 nm) and particles occasionally exceeding 100 nm, suggesting less uniformity. CpE-AgNPs, on the other hand, were mostly spherical to quasi-spherical within the range of 50–80 nm, with occasional rods. VeV-AgNPs were predominantly quasi-spherical with a mean size of 45.0 ± 8.5 nm, though occasional rodlike shapes were observed. As presented in Table 1, while all three extracts facilitated nanoparticle formation, *Dialium cochinchinense* extract appeared to produce smaller and more uniform particles compared to the other two.

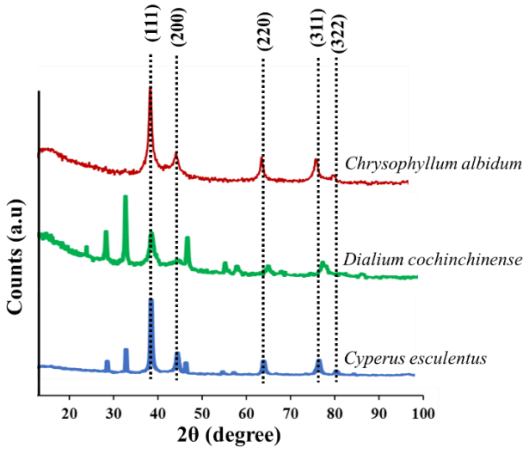

Figure 2. P-XRD pattern of prepared silver nanoparticles showing the various diffraction planes

Figure 2 presents the XRD patterns of the prepared silver nanoparticles. VeV-AgNPs, Alb-AgNPs and CpE-AgNPs all exhibited face-centred cubic (FCC) crystalline structures, as confirmed by XRD analyses showing characteristic diffraction peaks at 2θ values near 38°, 44°, 64°, 78° and 81° [43]. However, in the spectrum of CpE-AgNPs and VeV-AgNPs, additional peaks were observed. These peaks can be attributed to the crystallization of certain biomolecules in the extract solution on the prepared silver nanoparticles [44].

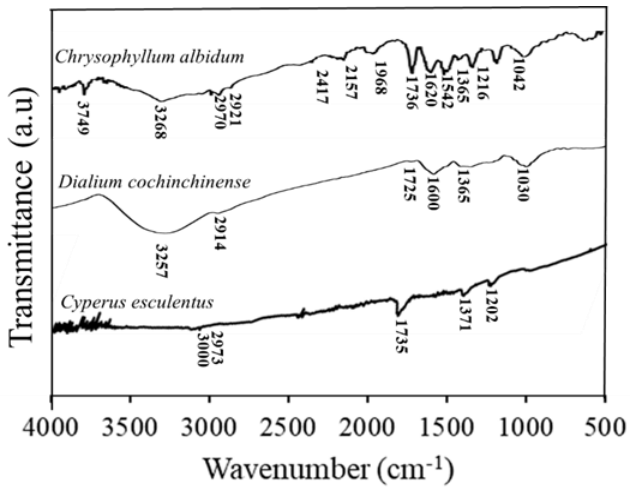

Figure 3. FTIR spectrum of the prepared silver nanoparticles

A key difference among the three systems was their reaction kinetics and functional group involvement. All the prepared silver nanoparticles showed rapid sunlight-mediated reduction of Ag^+ ions, with complete reactions occurring in about 5 minutes under sunlight compared to hours under ambient conditions. Nevertheless, CpE-AgNPs formed more slowly under room conditions, requiring up to 24 hours for complete reduction. This is likely due to the reliance on

amino acids such as aspartic and glutamic acids in the tuber extract as electron donors [35]. FTIR analyses of all three nanoparticles as illustrated in Figure 3, revealed bio-organic functional groups such as O–H, C=O, C–O, C=C and C–N, attached to the nanoparticle surfaces, which acted as capping and stabilizing agents [45].

The plasmonic absorption maxima were comparable but slightly varied as VeV-AgNPs absorbed at around 455 nm, CpE-AgNPs at ~450 nm, and Alb-AgNPs at ~434 nm, reflecting subtle differences in size distribution and surface chemistry.

3.2. Antibacterial Analyses of VeV-AgNPs, Alb-AgNPs and CpE-AgNPs

Alb-AgNPs exhibited significant antimicrobial effects across a broad range of bacterial and fungal pathogens. They demonstrated strong activity against *E. coli, K. pneumoniae, P. aeruginosa, S. aureus, B. subtilis, S. mutans, and C. albicans,* with minimum inhibitory concentration (MIC) values as low as 15.62 µg/mL for some strains. Notably, Alb-AgNPs outperformed silver nitrate ($AgNO_3$) in several cases, particularly against *E. coli and C. albicans.* Synergistic studies, as presented in Table 2, showed that Alb-AgNPs enhanced the activity of tetracycline against *K. pneumoniae, S. mutans, and B. subtilis,* as well as ciprofloxacin against MRSA and *P. aeruginosa*. This suggests that Alb-AgNPs are effective both as standalone antimicrobials and as enhancers of antibiotic action.

CpE-AgNPs demonstrated moderate antimicrobial activity compared to Alb-AgNPs and VeV-AgNPs. The MICs of CpE-AgNPs values ranged from 62.5 to 250 µg/mL, indicating that higher doses were required to achieve inhibition. Nevertheless, they exhibited consistent bactericidal action and fungicidal effects against *C. albicans*. The slower larger particle size may account for the relatively lower potency [46]. Interestingly, CpE-AgNPs still showed notable synergy with tetracycline (*against K. pneumoniae, S. mutans, and B. subtilis*) and with ciprofloxacin (against *P. aeruginosa*), indicating a role in combination therapy rather than as standalone potent agents. VeV-AgNPs were the most potent of the three nanoparticles. They displayed remarkably low MIC values, with as little as 3.9 µg/mL sufficient to inhibit *E. coli*. Their antimicrobial activity extended broadly to both Gram-positive and Gram-negative bacteria, as well as *C. albicans*. This high level of activity is attributed to their relatively small and uniform size [46]. In synergistic assays, VeV-AgNPs markedly improved the efficacy of ciprofloxacin across nearly all tested bacteria, showing strong potential as adjunct agents for antibiotic therapies.

Table 2. Antimicrobial studies (MIC and synergistic properties) of the prepared silver nanoparticles

AgNP	MIC Range (µg/mL)	Most Effective Against	Synergy
Alb-AgNPs	15.62 – 125	*E. coli*, *K. pneumoniae*, *P. aeruginosa*, *C. albicans*	Synergy with tetracycline (*K. pneumoniae*, *S. mutans*, *B. subtilis*); synergy with ciprofloxacin (MRSA, *P. aeruginosa*)
VeV-AgNPs	3.9 – 62.5	*E. coli*, broad-spectrum bacteria and *C. albicans*	Strong synergy with ciprofloxacin against most bacteria
CpE-AgNPs	62.5 – 250	*C. albicans*, moderate bacterial activity	Synergy with tetracycline (*K. pneumoniae*, *S. mutans*, *B. subtilis*); synergy with ciprofloxacin (*P. aeruginosa*)

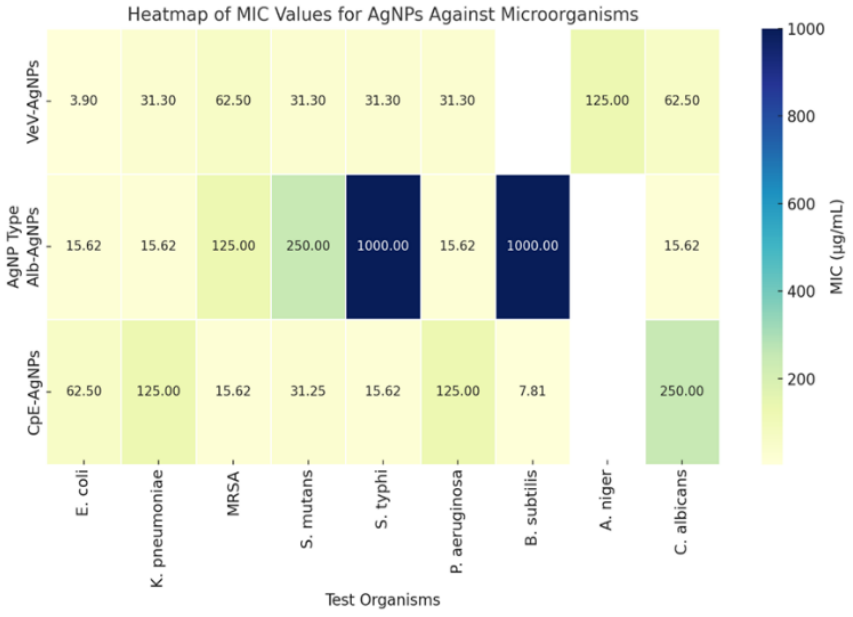

Figure 4. Heatmap showing the sensitivity of the prepared silver nanoparticles against tested microorganisms. Darker colours represent lower MICs

Figure 4 shows a comparison between the prepared nanoparticles. VeV-AgNPs clearly emerged as the most effective antimicrobial nanoparticles, owing to their smaller particle size [46], broad-spectrum potency, including the lowest MIC values recorded. Alb-AgNPs ranked second, demonstrating strong effects against a wide spectrum of pathogens and particularly excelling against *E. coli* and *C. albicans.* They also showed broader synergistic potential than CpE-AgNPs, though not as extensive as VeV-AgNPs. CpE-AgNPs, while less potent in direct antimicrobial action, still contributed meaningfully in combination studies, highlighting their value as synergistic enhancers rather than primary antimicrobial agents.

Figure 5 shows the comparative ranking of the silver nanoparticles (AgNPs). As shown in Figure 5, there is a clear difference in both coverage and potency across the three prepared silver nanoparticles. CpE-AgNPs demonstrated the broadest antimicrobial spectrum, outperforming the others against four organisms, including resistant strains such as MRSA and *S. typhi*, with a lowest MIC of 7.81 µg/mL. VeV-AgNPs exhibited exceptional potency against *E. coli* with the lowest overall MIC value (3.9 µg/mL), though their coverage was limited to two organisms. In contrast, Alb-AgNPs showed moderate coverage (three organisms) but consistently higher MIC values, indicating weaker antimicrobial activity overall.

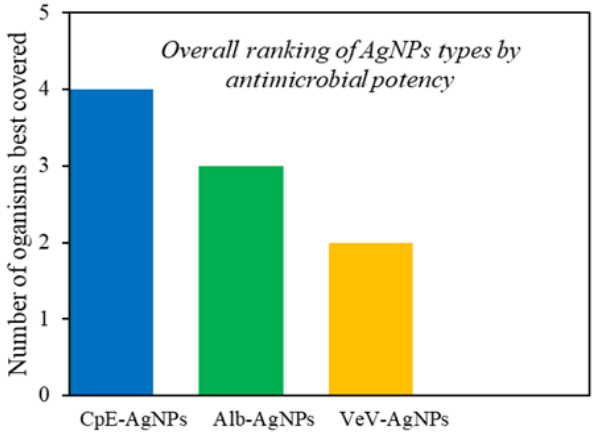

Figure 5. Ranking of prepared silver nanoparticles in terms of coverage

The versatility of CpE-AgNPs in terms of wide number of microorganisms inhibited may be attributed to the rich phytochemical profile of *Cyperus esculentus* tubers, which are known to contain high levels of phenolics, flavonoids, and tannins that act as strong reducing and stabilizing agents during nanoparticle synthesis [47]. These biomolecules likely contributed to the formation of smaller, more stable nanoparticles with enhanced surface reactivity, thereby increasing their antimicrobial potency (Dakal et al. 2016). In comparison, VeV-AgNPs, although highly effective against *E. coli*, may have produced nanoparticles with more selective activity due to differences in capping agents and metal-binding phytochemicals. The relatively weaker activity of Alb-AgNPs could be linked to lower concentrations or different types of secondary metabolites, resulting in less efficient nanoparticle formation and reduced antimicrobial efficacy. These observations support the hypothesis that the nature and concentration of plant-derived phytochemicals play a crucial role in determining nanoparticle characteristics and, ultimately, their biological performance [47].

3.3. Antibiofilm Properties of the Prepared Silver Nanoparticles

The CpE-AgNPs exhibited strong antibiofilm activity against a broad spectrum of microbes, including *S. mutans*, *MRSA*, *B. subtilis*, *P. aeruginosa*, *S. typhi*, and *C. Albicans* (Table 3). Remarkably, complete inhibition (100%) of *MRSA* and *S. mutans* biofilms was achieved at relatively low concentrations (125 µg/mL and 62.5 µg/mL, respectively), far lower than what was required by previously reported AgNPs. Against *P. aeruginosa* and *C. albicans*, 100% inhibition occurred only at higher concentrations (250 µg/mL), but even low doses yielded significant activity (>50% inhibition at <20 µg/mL). The order of sensitivity at 62.5 µg/mL was *S. mutans* > MRSA > *C. albicans* > *P. aeruginosa* > *S. typhi* > *B. subtilis*. This shows CpE-AgNPs are particularly potent against oral pathogens (*S. mutans*) and resistant bacteria (MRSA). Alb-AgNPs also displayed broad antibiofilm activity but were generally less potent than CpE-AgNPs. At the maximum tested concentration (250 µg/mL), inhibition ranged from ~54% (*B. subtilis*) to > 90% (*MRSA*). Against *S. typhi* and *C. albicans*, the inhibition was high (83% and 88% respectively), while for *S. mutans* it was more moderate (57%). Compared to CpE-AgNPs, Alb-AgNPs required higher concentrations to achieve significant inhibition, but their performance against *C. albicans* was notable. The sensitivity trend was MRSA > *S. typhi* > *C. albicans* > *S. mutans* > *B. subtilis*.

The VeV-AgNPs demonstrated the broadest and most versatile antibiofilm effect, showing activity against both biofilm formation and pre-formed biofilms. They were effective against *E. coli*, *K. pneumoniae*, *S. mutans*, *S. typhi*, *P. aeruginosa*, MRSA, *A. niger, and C. albicans*. Biofilm inhibition >99% was recorded against *E. coli*, *S. mutans*, and *A. niger*. At 250 µg/mL, the inhibition trend for newly formed biofilms was *S. mutans* > *E. coli* > *K. pneumoniae* > *S. typhi* > *P. aeruginosa* > MRSA, while for fungal strains it was *A. niger* > *C. albicans*. Even against pre-formed biofilms, VeV-AgNPs showed >89% reduction for *S. mutans*. This makes them more effective and versatile compared to both CpE-AgNPs and Alb-AgNPs.

Table 3 shows a comparison between the prepared nanoparticles; it is clear that their antibiofilm performance differs both in terms of potency and spectrum of activity. The CpE-AgNPs are remarkable for their strong inhibition at very low concentrations. For example, MRSA biofilms were completely suppressed at just 125 µg/mL, and *S. mutans* at only 62.5 µg/mL, showing that CpE-AgNPs are highly effective against these notoriously resilient microbes. This level of low-dose potency is far superior to many previously reported AgNPs, which often required doses in the milligram range to achieve similar effects [48]. Thus, CpE-AgNPs stand out as the most efficient nanoparticles when small amounts are considered.

Table 3. Antibiofilm performance of the prepared silver nanoparticles

Microorganism	CpE-AgNPs	Alb-AgNPs	VeV-AgNPs
MRSA	100% inhibition at 125 µg/mL; >50% at 1.96 µg/mL (very potent at low dose).	>90% inhibition at 250 µg/mL (strong, but needs higher concentration).	Effective, but less than CpE-AgNPs; not as low-dose potent.
S. mutans	100% inhibition at 62.5 µg/mL; >50% at 1.96 µg/mL (excellent potency).	57% inhibition at 250 µg/mL (moderate).	>99% inhibition; also reduces pre-formed biofilms by ~89% (broad activity).
B. subtilis	95% inhibition at 250 µg/mL drops sharply below that (weaker).	~54% inhibition at 250 µg/mL (low).	Effective, but less emphasized than *E. coli*/*S. mutans*.
S. typhi	77% inhibition at 250 µg/mL (moderate; less potent than others).	~83% inhibition at 250 µg/mL (strong).	Strong inhibition, >80%; also reduces pre-formed biofilms.
P. aeruginosa	100% inhibition at 250 µg/mL; >50% at 7.81 µg/mL (good).	Not tested.	Good inhibition; less effective than against *S. mutans*/*E. coli*.
E. coli	Not tested.	Not tested.	>99% inhibition at 250 µg/mL (excellent).
K. pneumoniae	Not tested.	Not tested.	Strong inhibition; >80% at 250 µg/mL.
C. albicans	100% inhibition at 250 µg/mL; 50% at 15.63 µg/mL (high potency).	~88% inhibition at 250 µg/mL (strong).	Inhibition observed; less than *A. niger* but effective.
A. niger	Not tested.	Not tested.	>99% inhibition at 250 µg/mL; best among fungi.

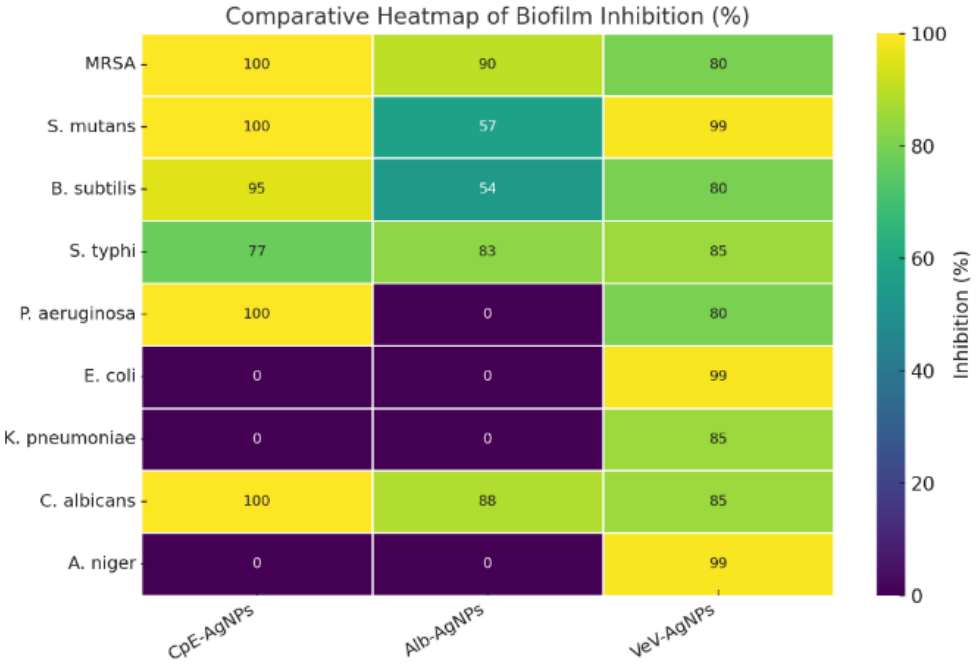

Figure 6. Heatmap showing the sensitivity of the prepared silver nanoparticles against biofilms of tested microorganisms. Darker colours represent lower MICs (in this case areas represented zero (0) was not tested for the said silver nanoparticles

By contrast, the Alb-AgNPs, while effective, generally required higher concentrations to exert significant inhibition. The maximum inhibition recorded for Alb-AgNPs ranged from around 54% for *B. subtilis* to over 90% for MRSA, with *S. typhi* (83%) and *C. albicans* (88%) also showing strong responses. Compared to CpE-AgNPs, Alb-AgNPs were less potent at lower concentrations but nonetheless provided consistent inhibition across both bacteria and fungi. This suggests that Alb-AgNPs may serve as reliable but moderate antibiofilm agents, particularly for *C. albicans* and *S. typhi*. The VeV-AgNPs, however, demonstrated the broadest and most versatile activity. Unlike CpE-AgNPs and Alb-AgNPs, which were mainly tested against a narrower set of pathogens, the VeV-AgNPs inhibited both the formation of biofilms and disrupted pre-formed biofilms across a wide range of organisms. They were especially powerful against *E. coli*, *S. mutans*, and *A. niger*, achieving nearly complete inhibition (>99%). Even when tested against pre-formed biofilms, traditionally much harder to treat, VeV-AgNPs retained high efficacy, showing almost 90% reduction in *S. mutans* biofilms at 250 µg/mL. This dual action highlights VeV-AgNPs as the most adaptable among the three.

A critical look at the performance of the prepared silver nanoparicles reveals that CpE-AgNPs dominate against *S. mutans* and MRSA at low doses, highlighting their clinical promise against oral pathogens and resistant strains. Alb-AgNPs perform comparatively better against *S. typhi* and *C. albicans*, though they lag in activity at low concentrations. VeV-AgNPs, in contrast, show a more universal spectrum, excelling not only against both bacteria and fungi but also

demonstrating the unique ability to reduce pre-formed biofilms, an advantage neither CpE-AgNPs nor Alb-AgNPs clearly achieved.

4. Conclusions

In this work, different silver nanoparticles, CpE-AgNPs, Alb-AgNPs and VeV-AgNPs biogenically prepared were compared to study their antimicrobial properties. This is important to rationalized the effect of surface functionalization on antimicrobial properties. In terms of effectiveness, VeV-AgNPs showed the most versatility, exhibiting ability to inhibit microbial growth even at a very low concentration. CpE-AgNPs, though with moderate antimicrobial action showed a broader antimicrobial spectrum against wider range of microorganisms highlighting their potential in therapeutic applications. Alb-AgNPs displayed reliable broad-spectrum activity with notable synergistic effects alongside conventional antibiotics. Collectively, these findings emphasize the role of phytochemical composition in shaping nanoparticle performance and support the development of green nanotechnology as a sustainable approach for addressing microbial resistance.

ACKNOWLEDGEMENTS

The authors acknowledge the contributions of Christopher Dawari and the University of Eastern Finland for SEM imaging.

REFERENCES

[1] A.M. Rabie, M. Abdalla, Forodesine and Riboprine Exhibit Strong Anti-SARS-CoV-2 Repurposing Potential: In Silico and In Vitro Studies, ACS Bio Med Chem Au. 2 (2022) 565–585. https://doi.org/10.1021/ACSBIOMEDCHEMAU.2C00039.

[2] W.A. Eltayb, M. Abdalla, A.M. Rabie, Novel Investigational Anti-SARS-CoV-2 Agent Ensitrelvir "S-217622": A Very Promising Potential Universal Broad-Spectrum Antiviral at the Therapeutic Frontline of Coronavirus Species, ACS Omega. 8 (2023) 5234–5246. https://doi.org/10.1021/ACSOMEGA.2C03881.

[3] A.M. Rabie, Two antioxidant 2,5-disubstituted-1,3,4-oxadiazoles (CoViTris2020 and ChloViD2020): successful repurposing against COVID-19 as the first potent multitarget anti-SARS -CoV-2 drugs, New J. Chem. 45 (2021) 761–771. https://doi.org/10.1039/D0NJ03708G.

[4] A.M. Rabie, Teriflunomide: A possible effective drug for the comprehensive treatment of COVID-19, Curr. Res. Pharmacol. Drug Discov. 2 (2021) 100055. https://doi.org/10.1016/J.CRPHAR.2021.100055.

[5] A.M. Rabie, W.A. Eltayb, Potent Dual Polymerase/Exonuclease Inhibitory Acti vities of Antioxidant Aminothiadiazoles Against the COVID-19 Omicron Virus: A Promising In Silico/In Vitro Repositioning Research Study, Mol. Biotechnol. 66 (2024) 592–611. https://doi.org/10.1007/S12033-022-00551-8/TABLES/3.

[6] A.M. Rabie, M. Abdalla, Evaluation of a series of nucleoside analogs as effective anticoronaviral-2 drugs against the Omicron-B.1.1.529/BA.2 subvariant: A repurposing research study, Med. Chem. Res. 32 (2023) 326–341. https://doi.org/10.1007/S00044-022-02970-3/FIGURES/6.

[7] A.M. Rabie, Efficacious Preclinical Repurposing of the Nucleoside Analogue Didanosine against COVID-19 Polymerase and Exonuclease, ACS Omega. 7 (2022) 21385–21396. https://doi.org/10.1021/ACSOMEGA.1C07095.

[8] A. Barapatre, K.R. Aadil, H. Jha, Synergistic antibacterial and antibiofilm activity of silver nanoparticles biosynthesized by lignin-degrading fungus, Bioresour. Bioprocess. 3 (2016) 1–13. https://doi.org/10.1186/s40643-016-0083-y.

[9] K.S. Siddiqi, A. Husen, R.A.K. Rao, A review on biosynthesis of silver nanoparticles and their biocidal properties, J. Nanobiotechnology. 16 (2018) 1–28. https://doi.org/10.1186/s12951-018-0334-5.

[10] S. Anees Ahmad, S. Sachi Das, A. Khatoon, M. Tahir Ansari, M. Afzal, M. Saquib Hasnain, A. Kumar Nayak, Bactericidal activity of silver nanoparticles: A mechanistic review, Mater. Sci. Energy Technol. 3 (2020) 756–769. https://doi.org/10.1016/j.mset.2020.09.002.

[11] N. Chandrasekhar, S.P. Vinay, Yellow colored blooms of argemone mexicana and turnera ulmifolia mediated synthesis of silver nanoparticles and study of their antibacterial and antioxidant activity, Appl. Nanosci. 7 (2017) 851–861. https://doi.org/10.1007/s13204-017-0624-5.

[12] C.O. Bamigboye, J.A. Amao, I.A. Fadiora, J.D. Adegboye, O.E. Akinola, A.A. Alarape, O.R. Oyeleke, E.A. Adebayo, Antioxidant and antimicrobial activities of nanosilver- mycomeat composite produced through solid state fermentation of tigernut waste and cassava pulp by Pleurotus pulmonarius, IOP Conf. Ser. Mater. Sci. Eng. 805 (2020) 012011. https://doi.org/10.1088/1757-899X/805/1/012011.

[13] J.C.S. Costa, P. Corio, L.M. Rossi, Catalytic oxidation of cinnamyl alcohol using Au-Ag nanotubes investigated by surface-enhanced Raman spectroscopy., Nanoscale. 7 (2015) 8536–43. https://doi.org/10.1039/c5nr01064k.

[14] G. Herrera, A. Padilla, S. Hernandez-Rivera, Surface Enhanced Raman Scattering (SERS) Studies of Gold and Silver Nanoparticles Prepared by Laser Ablation, Nanomaterials. 3 (2013) 158–172. https://doi.org/10.3390/nano3010158.

[15] B. Ankudze, A. Philip, T.T. Pakkanen, Controlled synthesis of high yield polyhedral polyethylenimine-capped gold nanoparticles for real-time reaction monitoring by SERS, Sensors Actuators B Chem. 265 (2018) 668–674. https://doi.org/10.1016/J.SNB.2018.03.088.

[16] F. Jelin, S. Selva Kumar, M. Malini, M. Vanaja, G. Annadurai, Environmental-Assisted green approach AgNPs by nutmeg (Myristica fragrans): Inhibition potential accustomed to pharmaceuticals, Eur. J. Biomed. Pharm. Sci. 2 (2015) 258–274.

[17] E. Vatandost, F. Chekin, S.A. Shahidi Yasaghi, Green synthesis of silver nanoparticles by pepper extracts reduction and its electocatalytic and antibacterial activity, Russ. J. Electrochem. 2016 5210. 52 (2016) 960–965. https://doi.org/10.1134/S102319351610013X.

[18] P. Khanna, A. Kaur, D. Goyal, Algae-based metallic nanoparticles: Synthesis, characterization and applications, J. Microbiol. Methods. 163 (2019) 105656.

https://doi.org/10.1016/J.MIMET.2019.105656.

[19] M. Gajbhiye, J. Kesharwani, A. Ingle, A. Gade, M. Rai, Fungus-mediated synthesis of silver nanoparticles and their activity against pathogenic fungi in combination with fluconazole, Nanomedicine Nanotechnology, Biol. Med. 5 (2009) 382–386. https://doi.org/10.1016/J.NANO.2009.06.005.

[20] D. Zhang, X.L. Ma, Y. Gu, H. Huang, G.W. Zhang, Green Synthesis of Metallic Nanoparticles and Their Potential Applications to Treat Cancer, Front. Chem. 8 (2020) 1–18. https://doi.org/10.3389/fchem.2020.00799.

[21] A. Krół, V. Railean-Plugaru, P. Pomastowski, B. Buszewski, Phytochemical investigation of Medicago sativa L. extract and its potential as a safe source for the synthesis of ZnO nanoparticles: The proposed mechanism of formation and antimicrobial activity, Phytochem. Lett. 31 (2019) 170–180. https://doi.org/10.1016/J.PHYTOL.2019.04.009.

[22] A. Ashraf, S. Zafar, K. Zahid, M. Salahuddin Shah, K.A. Al-Ghanim, F. Al-Misned, S. Mahboob, Synthesis, characterization, and antibacterial potential of silver nanoparticles synthesized from Coriandrum sativum L., J. Infect. Public Health. 12 (2019) 275–281. https://doi.org/10.1016/J.JIPH.2018.11.002.

[23] Z. Yu, J. Liu, H. He, Y. Wang, Y. Zhao, Q. Lu, Y. Qin, Y. Ke, Y. Peng, Green synthesis of silver nanoparticles with black rice (Oryza sativa L.) extract endowing carboxymethyl chitosan modified cotton with high anti-microbial and durable properties, Cellul. 2021 283. 28 (2021) 1827–1842. https://doi.org/10.1007/S10570-020-03639-Z.

[24] R. Tamileswari, M. Haniff Nisha, S.S. Jesurani, Green Synthesis of Silver Nanoparticles using Brassica Oleracea (Cauliflower) and Brassica Oleracea Capitata (Cabbage) and the Analysis of Antimicrobial Activity, Int. J. Eng. Res. Technol. 4 (2015) 1071–1074. www.ijert.org (accessed March 27, 2022).

[25] S.T. Shah, I.P. Sari, D.H.Y. Yanto, Z.Z. Chowdhury, M.N. Bashir, I.A. Badruddin, M. Hussien, J.S. Lee, Nature's nanofactories: biogenic synthesis of metal nanoparticles for sustainable technologies, Green Chem. Lett. Rev. 18 (2025) 1–42. https://doi.org/10.1080/17518253.2024.2448171.

[26] F. Benyettou, R. Rezgui, F. Ravaux, T. Jaber, K. Blumer, M. Jouiad, L. Motte, J.C. Olsen, C. Platas-Iglesias, M. Magzoub, A. Trabolsi, Synthesis of silver nanoparticles for the dual delivery of doxorubicin and alendronate to cancer cells, J. Mater. Chem. B. 3 (2015) 7237–7245. https://doi.org/10.1039/C5TB00994D.

[27] S.H. Lee, B.H. Jun, Silver Nanoparticles: Synthesis and Application for Nanomedicine, Int. J. Mol. Sci. 20 (2019) 865. https://doi.org/10.3390/IJMS20040865.

[28] G.S. Tkemaladze, K.A. Makhashvili, Climate changes and photosynthesis, Ann. Agrar. Sci. 14 (2016) 119–126. https://doi.org/10.1016/J.AASCI.2016.05.012.

[29] M.I. Skiba, V.I. Vorobyova, Synthesis of Silver Nanoparticles Using Orange Peel Extract Prepared by Plasmochemical Extraction Method and Degradation of Methylene Blue under Solar Irradiation, Adv. Mater. Sci. Eng. 2019 (2019) 1–8. https://doi.org/10.1155/2019/8306015.

[30] M. Zia, S. Gul, J. Akhtar, I. Ul Haq, B.H. Abbasi, A. Hussain, S. Naz, M.F. Chaudhary, Green synthesis of silver nanoparticles from grape and tomato juices and evaluation of biological activities, IET Nanobiotechnology. 11 (2017) 193–199. https://doi.org/10.1049/IET-NBT.2015.0099.

[31] F.U. Asoiro, S.L. Ezeoha, G.I. Ezenne, C.B. Ugwu, Chemical and Mechanical Properties of Velvet Tamarind Fruit (Dalium Guineese), Niger. J. Technol. 36 (2017) 252–260.

[32] O. Zacchaeus, A. Iyadunni, A. Johnson, U. Daubotei, Black Velvet Tamarind : Phytochemical Analysis, Antiradical and Antimicrobial Properties of the Seed Extract for Human Therapeutic and Health Benefits, J. Phytopharm. 10 (2021) 249–255. https://doi.org/10.31254/phyto.2021.10406.

[33] U.E. Odoh, Establishment of Quality Parameters and Pharmacognostical Profiling of Dialium guinneense, World J. Innov. Res. 8 (2020) 47–46.

[34] I.A. Ajayi, A.A. Raji, E.O. Ogunkunle, Green synthesis of silver nanoparticles from seed extracts of Cyperus esculentus and Butyrospermum paradoxum, IOSR J. Pharm. Biol. Sci. Ver. I. 10 (2015) 2319–7676. https://doi.org/10.9790/3008-10417690.

[35] B. Ankudze, V.B. Samlafo, Repeated Use of Cyperus esculentus Tubers, Towards Sustainable Green Synthesis of Silver Nanoparticles, BioNanoScience 2022. 12 (2022) 1150–1157. https://doi.org/10.1007/S12668-022-01032-7.

[36] B. Ankudze, D. Neglo, Green synthesis of silver nanoparticles from peel extract of Chrysophyllum albidum fruit and their antimicrobial synergistic potentials and biofilm inhibition properties, BioMetals. 36 (2022) 865–876. https://doi.org/10.1007/S10534-022-00483-5/METRICS.

[37] B. Ankudze, D. Neglo, F. Nsiah, Green synthesis of silver nanoparticles from discarded shells of velvet tamarind (Dialium cochinchinense) and their antimicrobial synergistic potentials and biofilm inhibition properties, BioMetals. 37 (2024) 143–156. https://doi.org/10.1007/S10534-023-00534-5/METRICS.

[38] N.K. Ayisi, R. Appiah-Opong, B. Gyan, K. Bugyei, F. Ekuban, Plasmodium falciparum : Assessment of Selectivity of Action of Chloroquine, Alchornea cordifolia, Ficus polita, and Other Drugs by a Tetrazolium-Based Colorimetric Assay, Malar. Res. Treat. 2011 (2011) 1–7. https://doi.org/10.4061/2011/816250.

[39] E.W. Nester, D.. Anderson, C.E. Roberts Jr, N.N. Pearsall, T. Nester, D. Hurley, Microbiology A human perspective, 4th Editio, McGraw-Hill, Boston., New York, USA, 2004. https://www.scirp.org/(S(lz5mqp453edsnp55rrgjct55))/reference/ReferencesPapers.aspx?ReferenceID=1856478 (accessed April 28, 2022).

[40] A. Khodavandi, F. Alizadeh, F. Aala, Z. Sekawi, P.P. Chong, In vitro investigation of antifungal activity of allicin alone and in combination with azoles against Candida species, Mycopathologia. 169 (2010) 287–295. https://doi.org/10.1007/S11046-009-9251-3.

[41] L.C. Nascimento Da Silva, J. Messias Sandes, M.M. De Paiva, J.M. De Araújo, R.C.B.Q. De Figueiredo, M.V. Da Silva, M.T.D.S. Correia, Anti-Staphylococcus aureus action of three Caatinga fruits evaluated by electron microscopy, Nat. Prod. Res. 27 (2013) 1492–1496. https://doi.org/10.1080/14786419.2012.722090.

[42] C.G. Pierce, P. Uppuluri, A.R. Tristan, F.L. Wormley, E. Mowat, G. Ramage, J.L. Lopez-Ribot, A simple and reproducible 96-well plate-based method for the formation of fungal biofilms and its application to antifungal susceptibility

testing, Nat. Protoc. 3 (2008) 1494–1500. https://doi.org/10.1038/NPORT.2008.141.

[43] N. Krithiga, A. Rajalakshmi, A. Jayachitra, Green Synthesis of Silver Nanoparticles Using Leaf Extracts of Clitoria ternatea and Solanum nigrum and Study of Its Antibacterial Effect against Common Nosocomial Pathogens, J. Nanosci. 2015 (2015) 1–8. https://doi.org/10.1155/2015/928204.

[44] M. Vanaja, G. Annadurai, Coleus aromaticus leaf extract mediated synthesis of silver nanoparticles and its bactericidal activity, Appl. Nanosci. 3 (2013) 217–223. https://doi.org/10.1007/s13204-012-0121-9.

[45] J. Huang, Q. Li, D. Sun, Y. Lu, Y. Su, X. Yang, H. Wang, Y. Wang, W. Shao, N. He, J. Hong, C. Chen, Biosynthesis of silver and gold nanoparticles by novel sundried Cinnamomum camphoraleaf, Nanotechnology. 18 (2007) 105104. https://doi.org/10.1088/0957-4484/18/10/105104.

[46] T.T.T. Vi, S.R. Kumar, Y.T. Huang, D.W. Chen, Y.K. Liu, S.J. Lue, Size-dependent antibacterial activity of silver nanoparticle-loaded graphene oxide nanosheets, Nanomaterials. 10 (2020) 1–18. https://doi.org/10.3390/nano10061207.

[47] I. Santos, A. Sousa, A. Vale, F. Carvalho, E. Fernandes, M. Freitas, Protective effects of flavonoids against silver nanoparticles-induced toxicity, Arch. Toxicol. 99 (2025) 3105–3132. https://doi.org/10.1007/s00204-025-04068-2.

[48] A.A. Alyousef, M. Arshad, R. AlAkeel, A. Alqasim, Biogenic silver nanoparticles by Myrtus communis plant extract: biosynthesis, characterization and antibacterial activity, Biotechnol. Biotechnol. Equip. 33 (2019) 931–936. https://doi.org/10.1080/13102818.2019.1629840.